Martin Marietta Laboratories

MARTIN MARIETTA

MML TR 94-12

Thin-Film Model Studies of Interfacial Reactions in Intermetallic Matrix Composites

N00014-91-C-0168

Final Report

June 1, 1991 - May 30, 1994

Submitted to:

Office of Naval Research
800 North Quincy Street
Arlington, VA 22217-5000

Submitted by:

M. Nathan and J.S. Ahearn
Martin Marietta Laboratories • Baltimore
1450 S. Rolling Road, Baltimore, MD 21227

August 1994

MML TR 94-12

Thin-Film Model Studies of Interfacial Reactions in Intermetallic Matrix Composites

Final Report

June 1, 1991 — May 30, 1994

Submitted to:

Office of Naval Research
800 North Quincy Street
Arlington, VA 22217-5000

Submitted by:

M. Nathan and J.S. Ahearn
Martin Marietta Laboratories • Baltimore
1450 S. Rolling Road, Baltimore, MD 21227

August 1994

TABLE OF CONTENTS

I. INTRODUCTION

The study of interfacial reactions in metal or intermetallic matrix composites goes back to the early sixties, when major programs funded by the US Air Force seeked to develop high temperature composites. An excellent status summary on the subject was given by Metcalfe[1] in 1974. At that time, models of the interface[2] and its physical and chemical aspects[3], recognized the importance of the scale of the reaction, in particular the "under 10000Å zone", in determining composite properties. However, the methodology of studying interfacial reactions on this scale was largely restricted to electron microscopy (SEM and TEM) of specimens prepared from bulk composites, the main exception being studies of film-coated fibres[4,5]. The resolution in most cases was limited, and no special effort was made to define the reaction products on a scale smaller than a fraction of a micron. With the introduction of surface techniques (AES and XPS) and analytical electron microscopy(AEM), and developments in microelectronics processing which required detailed knowledge of metal/Si or metal/SiO_2 reactions, model studies in which a thin film of one material was deposited on a bulk substrate became popular. These studies provided a detailed picture of such processes as oxidation and diffusion on an atomic scale, but left largely unanswered the question of the link betweenthem and real-life composite properties, a link which is still by-and-large missing. More recently, the interest in intermetallic based composites has added complexity to the study of nanometer-scale interfacial reactions, which have reverted to being carried out almost exclusively with TEM. The main drawback of standard TEM (which views an interface perpendicular to its normal) is that it provides great detail of a very minute part of the interface. This can be alleviated in part by using TEM (mainly in diffraction mode) on a layered thin-film model system with the beam parallel to the interface normal, thus acquiring data from a much larger area without significantly sacrificing resolution. Since the interface is now buried at a depth of a few hundred Å, it can be expected also to behave more like a real composite interface, in contrast with the situation present in most surface studies. It must be pointed out however that the layered film system differs in microstructure, possibly in chemistry and certainly in its formation history from a bulk composite. This, and the possible introduction of artifacts during thermal treatments used to induce nanometer interfacial reactions in the films, must be considered in evaluating thin-film model results.

The issue of interfacial reactions between matrix and reinforcement can be viewed in terms of chemical compatibility. As generally understood, "compatibility" implies chemical inertness and therefore a lack of reaction at the interface. However, although large scale reactions are clearly deleterious to composite properties, the existence of a nanoscale reaction may in fact be necessary for good bonding. The main IMC systems being currently evaluated for high temperature applications are based on nickel and titanium aluminides. The chemical compatibility of TiAl and NiAl matrices with various reinforcements has been calculated [6,7] using up-to-date thermodynamic data. These calculations can at best be relied upon to predict bulk behavior, i.e. "macroscopic" reactivity, and eliminate clearly incompatible systems, in which extensive reactions are highly likely to occur. Most "borderline" or compatible systems will still have to be tested experimentally. The purpose of this program was to obtain important information on the interfacial reactions in both (predicted) compatible and incompatible systems, by using a novel approach of modelling bulk IMC reactions experimentally with thin layered films.

In addition to being chemically compatible, reinforcements should be closely matched in their thermal expansion coefficient (TCE) with the matrix, and available commercially. Only a few materials fulfill all conditions vs TiAl and NiAl[6,7]. We will start with NiAl IMC's. Misra[6] indicates that of all chemically compatible reinforcements, only La_2O_3 , MgO, cubic ZrO_2 and $CaZrO_3$ are closely matched in TCE with NiAl at 827°C. The difference between the TCE of MgO (15.2×10^{-6} C^{-1}) and that of NiAl (~16×10^{-6} C^{-1}) is about 5%. Interestingly, there are no reports in the literature on the NiAl-MgO composite system, possibly because it is expected to be unstable in dynamic environments, which are predicted to bring about the evaporation of Mg[6]. We therefore concentrated on Al_2O_3, ZrO_2 and MgO for NiAl and Al_2O_3 and TiB_2 for TiAl. We also investigated the TiAl/TiC system, predicted to be incompatible. The following report basically summarizes the results published in four papers[8-11] as well as unpublished results.

II. BASIC PROCEDURE

A. General

The basic idea of modelling a reinforcement R (e.g fiber)/matrix M interface with layered thin-films is illustrated in Fig. 1. If one considers only the narrow region around the interface itself, the main objective is to be able to reproduce the reactions occuring during composite formation or use at elevated temperatures, and to investigate them with ease, preferably with high resolution. This can be done with self-supporting thin layered films which provide a very large area of interface sandwiched between materials identical to those in bulk composites. Reaction caused by thermal annealing can be observed and characterized with electron microscopy/diffraction, as well as with surface techniques such as x-ray photoelectron spectroscopy (XPS).

B. The Thin-Film Technique

The technique is illustrated in Fig. 2. Layered thin films are electron beam (E-beam) evaporated in a high vacuum system onto either Formvar- or carbon-coated molybdenum electron microscope grids. After deposition, the Formvar is removed and the grids are annealed under relatively well controlled time/temperature conditions in a rapid thermal annealing (RTA) system. The grids can be examined by TEM after annealings as short as 1-2 sec and as long as 5 min at temperatures between 200 and 1250°C. Repeating the annealing/examination sequence provides many data points, each including the microstructure, phases present (from diffraction patterns) and, in some cases, kinetics (from grain growth)[12]. "Sandwiches" of films simulating R/M/R interfaces with varying R/M ratios and incorporating thin diffusion barriers can be deposited without breaking the vacuum. A sequential deposition of e.g Ni/Al or Ti/Al with thickness ratios calculated to give a particular stoichiometry, followed by a low temperature reaction, forms an intermetallic M layer. The low temperature in this step prevents a reaction between the outer layer of M and the R layer from taking place. In each case, separate M and R specimens were also procesed together with the R/M/R sandwich, and served as "baseline" specimens.

Specific experimental conditions regarding each M/R system studied can be found in references [8-11]. For example, Ti/Al/Al_2O_3 films were deposited by e-beam evaporation in an ultrahigh vacuum system with a base pressure of $5x10^{-8}$ torr. Pressures during evaporation were no higher than $2x10^{-7}$ torr for the Al and Ti films, and up to 10^{-6} torr for Al_2O_3. The latter was evaporated from polycrystalline chunks. The substrates were oxidized Si wafers and sapphire. The films-on-grid and on Si (deposited simultaneously and shown in Fig. 3a), were symmetrical, i.e., the Ti/Al layers were sandwiched between two 300Å- thick Al_2O_3 films with an Al thin layer adjacent to each Al_2O_3 film. The stacks on sapphire provided a nonsymmetrical structure, Fig. 3b, with an Al_2O_3 (film)/aluminide interface on one side and a sapphire/aluminide interface on the other. This arrangement allowed for a direct chemical comparison of Al_2O_3 films and sapphire, and for comparison of their respective reactions with the same aluminide. Other aluminide/R film stacks were prepared in a similar fashion. For example, the Ni/Al sequential deposition layer thicknesses are given in Table 1.

III. RESULTS

A. The NiAl/MgO System

1. Electron Microscopy

Figure 4 shows the SAD patterns of the as-deposited films. The MgO/Al/Ni film exhibits, as-expected, Al, Ni and MgO reflections. The standard Al/Ni specimen shows only Al and Ni reflections. In contrast with Al_2O_3[8], room-temperature deposited MgO is crystalline and its pattern matches well the periclase (JCPDS #4-829) phase[13]. Figure 5 shows the patterns after RTA at 300°C for 100s. The MgO/Al/Ni film consists now of very fine grained (solid diffraction lines) aluminide. Using the internal MgO lines for calibration, the measured spacings of the additional solid lines (indicated by arrows) are 4.89, 3.48, 2.87, 2.01, 1.42 and 1.17A, which match very well Al_3Ni_2 (JCPDS #14-648). This a slightly more Al-rich phase than expected from the multilayer stoichiometry. Note that since the last four lines also match very well NiAl (JCPDS #2-1261 or 20-19), it is impossible to state unequivocally that the aluminide phase is not NiAl, and it may well be that both Al_3Ni_2 and NiAl coexist in the film. Nevertheless, because all lines are accounted for, it is clear that the aluminide forms at low temperature without a significant reaction between the individual layers (and particularly Al) and MgO. When the starting stoichiometry is changed to 55%Ni-45%Al, the 300°C SAD pattern shows clearly only NiAl and MgO, and after subsequent annealings the results are identical to those in 50% Al films.

The Al/Ni film shows Ni_3Al (JCPDS #9-97) and gamma-Al_2O_3 (JCPDS #10-425) lines, while the MgO film is unchanged after the same RTA at 300°C. Although having an overall Al/Ni ratio identical to MgO/Al/Ni, oxidation of its external Al layers, possibly by residual oxygen in the RTA chamber, deprives the film of enough Al so that Ni_3Al forms instead of Al_3Ni_2 or NiAl (a simple calculation[8] shows that without the 100Å of the two external Al layers, the stack stoichiometry should be Ni_3Al). Formation of a metastable Al_2O_3 phase on NiAl in early oxidation stages is well established[14].

An additional RTA at 800°C for 300s yields the SAD patterns shown in Fig. 6, with their d-spacings listed in Table 2. Through comparison with the two standard films and the 300°C data, it is evident that a rather limited reaction took place. The arrows in the MgO/Al/Ni film point to the Al_3Ni_2 (NiAl) lines, still visible and quite strong.

New dotted rings indicate the presence of a minor new phase. As shown in Table 2, this phase is Ni_3Al. There is no evidence of Al_2O_3 being present. The presence of a weak line with d=4.68A indicates that a minor amount of the spinel phase, $MgAl_2O_3$ (JCPDS #21-1152) has formed. Its presence at the interface between the aluminide and the top MgO layer is confirmed by XPS (see below). The standard Al/Ni film is practically unchanged from 300°C. The standard MgO film shows an unidentified secondary phase, with lines which do not match any known magnesium oxide phase. Note (below) that this phase becomes dominant at 1000°C. We conclude that the nickel aluminide/MgO system compares favourably with systems such as Al_2O_3 /NiAl, and is more compatible at this temperature than other IMC's. Specifically, TiAl/MgO films annealed under identical conditions show no trace of TiAl, due to its total consumption in the reaction[15].

Further RTA at 1000°C for 100s yields the patterns and microstructures shown in Fig.7, and listed in Table 3. The MgO/Al/Ni film exhibits a number of clear semi-solid rings which match lines seen at 800°C. It is tempting to attribute these to the same phases (i.e. NiAl and MgO), in which case the conclusion is that the two are compatible even at 1000°C. On the other hand, all lines match quite well a spinel phase, either $NiAl_2O_4$ (JCPDS #10-339) or $MgAl_2O_4$. There is also extensive Ni agglomeration in the form of "globules" of material with diameters in the 0.2 - 1 μm range, in both MgO/Al/Ni and Al/Ni films. These globules also appear in Al_2O_3/Al/Ni and ZrO_2/Al/Ni but not in SiC/Al/Ni films [15], and are similar to the Ni globules in Ni/C reactions [12]. The Ni segregation implies that NiAl has broken up, freeing Ni. The presence of a spinel and free Ni points to a reaction such as

$$2NiAl + 4MgO \rightarrow NiAl_2O_4 + Ni + 4Mg \quad (1)$$

or

$$2NiAl + 4MgO \rightarrow MgAl_2O_4 + 2Ni + 3Mg \quad (2)$$

The molecular ratio of MgO/NiAl, taking a total of 600Å MgO and the thicknesses of the individual constituents of NiAl is roughly 1.77[8]. Given uncertainties in phase identification and in layer thicknesses, the above reactions can be reasonably considered balanced. Reaction (2) explains better the large amount of material in the Ni globules, and requires less free Mg to "disappear" from the film. The MgO film exhibits an excellent polycrystalline pattern which, however, does not match any standard Mg oxide file. The identity of this $Mg(O_x)$ phase remains a mystery; it could

be a new Mg-deficient, high-temperature MgO phase, possibly induced by the evaporation of Mg from the film. The small grained phase also appears in a MgO/Al/Ni film annealed separately only at 1000°C for 100s. Its similar texture in the two films is an indication that the changes in the MgO are partially independent of the presence of the aluminide.

The Al/Ni film is completely oxidized, with an extremely strong (440) gamma-Al_2O_3 line plus minor amounts of unidentified phases (one of which may well be $NiAl_2O_4$, since a few lines seem to overlap the main lines in the MgO/Al/Ni film). The absence of the (440) gamma-Al_2O_3 line in MgO/Al/Ni films means that NiAl oxidation due to residual oxygen in the annealing chamber is a much slower process than the MgO/NiAl interfacial reaction. In other words, artifacts introduced by oxygen diffusion through the MgO film to the MgO/NiAl interface do not affect significantly our results.

2. XPS

XPS depth profiles are useful mainly at lower temperatures, where the interaction of MgO with the SiO_2/Si substrate is limited. Profiles of a 300°C annealed film, and the same film after 800°C and 1000°C annealings are shown in Fig. 8. After 300°C, Fig. 8a, one sees clearly the MgO/"NiAl"/MgO sandwich atop the SiO_2 layer. The bottom (closer to SiO_2) MgO/Al interface is very sharp, while the top one is much broader, due to partial Al oxidation during the evaporation of MgO. The apparent Ni segregation to the sides of the Al/Ni multilayer structure is puzzling, and may be due in part to some artifact of the sputtering process, as well as due to the Al oxidation at the top interface. Note however that the average Al/Ni layer stoichiometry is indeed close to equiatomic. The MgO stoichiometry, calculated after calibrations with MgO crystals, is also close to the expected 1:1.

After exposure at 800°C, Fig. 8b, an interfacial reaction between MgO and NiAl is clearly visible. Limiting ourselves to the top interface in order to avoid artifacts introduced by the MgO/SiO_2 reaction, we see the formation of a wide Mg-O-Al region, which in accord with the SAD data is probably composed of the spinel $MgAl_2O_4$. The top MgO layer is still largely intact, but contains about 10% Al, which has diffused out out of the aluminide. The outdiffusion of Ni is negligible, in marked contrast with the findings of Bobeth et al[16], who identified Ni as the major diffusant out of Ni_3Al in an early oxidation stage. We submit that this contradiction is due to the different aluminide stoichiometry, and possibly due to the different microstructures. It seems

clear though that with increased Al content and with polycrystalline aluminide, Al and not the noble component will in fact be the first major diffusing species at the aluminide-oxide interface, as seen also in $TiAl/Al_2O_3$ reactions[8], and in other studies[17]. This has obvious implications for the choice of a diffusion barrier, which, if required, should target Al and not the noble component. It is also worthwhile noting that oxygen diffusion into the aluminide occurs concurently, as it does in $TiAl/Al_2O_3$ reactions[7].

The XPS profile of the 1000°C annealed film, Fig.8c, is not very instructive due to the extensive film-substrate reaction, which complicates tremendously the interpretation. This artifact can be eliminated of course by using MgO as a substrate, an experiment which has not been carried out. Nevertheless, some aspects of the MgO/NiAl reaction are clear: first, Mg has disappeared from the film, and this is not due to its diffusion into the substrate. Thus, the issue raised by Misra regarding Mg evaporation in a dynamic environment is confirmed. Second, the constant, low concentration of Ni, can best be explained by its existence in the form of globules distributed throughout the film, since once the distinct layer structure has broken up, phases coexisting side-by-side would give rise to a "smeared-out" depth profile. A direct comparison with the TEM results is of course impossible, but a certain conclusion is that the approximately 500Å thick aluminide layer has disintegrated.

B. The $NiAl/Al_2O_3$ and $NiAl/ZrO_2$ Systems

The preparation of the thin-film specimens and the experimental procedure are detailed in ref. 9. After 300s at 300°C, an Ni-Al reaction forms an aluminide (either Al_3Ni_2 or NiAl) layer, about 400-500Å thick. The aluminide layer, sandwiched between 300Å-thick Al_2O_3 or ZrO_2 layers reacts with them at high temperatures. Figure 9 shows the 300, 800 and 1000°C SAD patterns of $NiAl/Al_2O_3$ films, and Table 4 lists their d-spacings. At 300°C, the pattern is clearly that of Al_3Ni_2(JCPDS card #14-648), with no Al_2O_3 lines visible, since the as-deposited Al_2O_3 film is amorphous[8]. Further RTA at 800°C for 5 minutes leads to the decomposition reaction

$$Al_3Ni_2 \rightarrow 2NiAl + Al$$

and the crystallization of the alumina layer to gamma-Al_2O_3. The NiAl lines (dotted) and the gamma-Al_2O_3 lines (solid) are seen clearly in the figure. It is quite possible that Al_3Ni_2 decomposes due to oxidation involving residual oxygen in the annealing chamber which diffuses to the interface through Al_2O_3. As shown in the NiAl/MgO study, this oxidation is also evident in Al/Ni baseline films which are not sandwiched between Al_2O_3 layers. These layers therefore play no role at 800°C, and we conclude that there is no interfacial reaction between Al_3Ni_2 and Al_2O_3, **and that the interface is more stable than in NiAl/MgO thin films, where under identical conditions a reaction forms Ni_3Al and a spinel.**

Upon additional RTA at 1000°C for 100s,the pattern changes drastically,and is identical to that of a 1000°C annealed baseline Al_2O_3 film. This means that NiAl has oxidised and decomposed into its constituents, probably through an intermediate reaction

$$3NiAl + 3O \rightarrow Ni_3Al + Al_2O_3$$

leading to

$$Ni_3Al \rightarrow 3Ni + Al$$

The Ni agglomerates in globules, Fig. 10a, identical in size and shape to Ni agglomerates in a baseline Ni/Al film, Fig. 10b. The Al oxidises, or evaporates from the exposed surfaces. The transient oxidation of bulk NiAl at these temperatures is known to form gamma-Al_2O_3[14]. It is worth noting that the Al_2O_3 layer is continuous, with no voids of the type seen in the NiAl/ZrO_2 specimen (see below). The Al_2O_3 which forms in the baseline Ni/Al film is also continuous. These observations suggest that the oxidation is most likely due to residual O in the gas. Therefore, there is no true interfacial reaction between NiAl and Al_2O_3, and the two can be considered compatible, in agreement with bulk composite results reviewed in ref[18].

The SAD patterns of NiAl/ZrO_2 films after RTA at 300, 800 and 1000°C are shown in Fig. 11, and their d-spacings listed in Table 5. The microstructure at 1000°C is also shown. They can be compared with the patterns of a baseline 500Å-thick ZrO_2 film in Fig. 12. Both NiAl and tetragonal (t)-ZrO_2 (#34-1084) lines are evident in the 300°C films. NiAl may have formed instead of Al_3Ni_2 due to small differences in the Al/Ni ratio in the NiAl/ZrO_2 and NiAl/Al_2O_3 films.

The 800°C pattern contains all the lines seen at 300°C plus faint reflections of very small grained ZrO (#20-684) as well as reflections of very large grained Ni_3Al areas. This indicates a limited oxidation of NiAl, with some O probably coming from ZrO_2. Further annealing at 1000°C causes the disappearence of NiAl and Ni_3Al, the formation of Ni globules, and the transformation of t-ZrO_2 to monoclinic (m)-ZrO_2. In contrast with NiAl/Al_2O_3 and NiAl/MgO films,these films exhibit rather large voids in the ZrO_2 layers. The voids are not due to the t→m ZrO_2 transformation, which is known to be diffusionless[19] and do not appear in the baseline ZrO_2 film. Rather, they result from the decomposition of part of the ZrO_2 layer during reaction with Ni_3Al. **The NiAl/ZrO_2 system is therefore judged to be less stable than both NiAl/MgO and NiAl/Al_2O_3.** Note that as in NiAl/MgO, and unlike in NiAl/Al_2O3, there is no trace of gamma-Al_2O_3 at 1000°C, as expected if the free Al has evaporated.

Another interesting aspect of this reaction is its apparent effect on the crystallization of ZrO_2. The as-deposited ZrO_2 is amorphous in both NiAl/ZrO_2 and ZrO_2 films. The baseline ZrO_2 film crystallizes in the monoclinic structure as expected[20]. However, in the NiAl/ZrO_2 film the structure up to 800°C is tetragonal, transforming to m-ZrO_2 at 1000°C. The existence of t-ZrO_2 at a temperature much lower than the m→t transformation temperature of ca. 1170C[20] indicates that ZrO_2 is "stabilized" by NiAl. Its nucleation pattern is "inverted", the phase sequence with increasing temperature being amorphous ZrO_2→t-ZrO_2→m-ZrO_2.

Some of the effects seen in these films are obviously exagerated in comparison with bulk interfaces. For example, the agglomeration of Ni and the evaporation of Al, both involving fast diffusion paths, would probably be absent in bulk IMC's. However, when different thin-film model systems are compared with each other, we can still see a "stability ranking", one which we expect will extend to bulk composites. **As reinforcements in NiAl-based IMC's, Al_2O_3 would rank as most stable, followed by MgO. ZrO_2 rates as less stable than both.**

C. The TiAl/Al_2O_3 System

As mentioned in chapter I, among IMC's, the Ti aluminide (particularly gamma-TiAl) - Al_2O_3 system is quite promising for two reasons: excellent coefficient of thermal expansion (CTE) match and chemical compatibility between TiAl and Al_2O_3[7]. Bulk

studies show that aluminides with greater than or equal to 50% at. Al do not react with alumina[7,21,22], whereas for Al-poor (<50%) aluminides there is no consensus. For example, Misra[7] found that they do react; others[21,22] found that they do not. In thin films, the reports focus almost exclusively on Ti/alumina reactions; a good summary is given by Selverian et al[23]. The general view is that Ti film/bulk (crystalline) Al_2O_3 reactions form Ti_3Al and a Ti oxide[24], whereas thin film Ti/amorphous Al_2O_3 reactions form AlTi, TiO and Ti_2O[25]. Recent thermodynamic calculations of oxide stability in the Ti-Al-O system[26] indicate that at temperatures between 700°C-1100°C, Al_2O_3 would be unstable in alloys with compositions in the two-phase region Ti_3Al/TiAl. The scarcity of experimental data is one reason for the rather cloudy picture of Ti aluminide/alumina reactivity. Another is the poor resolution of most probing techniques with the exception of surface techniques [23,27] and high-resolution electron microscopy. The reactivity is thus defined by "macro" reactions (on a micron scale), while interfacial nanometer-scale reactions generally go undetected in supposedly "nonreactive" couples.

The experimental details of specimen preparation and annealings are given in ref. 8. Aluminide films with 30, 50 and 70% (atomic) Al were prepared and named Ti30Al, Ti50Al and Ti70Al respectively (see Fig. 3). Unlike in the rest of this study, a special "sandwich" of sapphire/TiAl/Al_2O_3 was also prepared, in order to follow both TiAl/(amorphous)Al_2O_3 and TiAl/sapphire reactions.

The diffraction patterns of all as-deposited films (see e.g Ti50Al in Fig. 13a) indicate the presence of polycrystalline Ti and Al, with ring intensities varying according to the relative amounts of the two materials. E-beam evaporated Al_2O_3 films are amorphous (a-Al_2O_3). Figure 14 shows the XPS profile and the Al2p and O1s scans of the as-deposited Ti50Al' (a-Al_2O_3/Ti+Al/sapphire). The atomic ratio O/Al in the Al_2O_3 film and in the sapphire is almost identical, as is the Al-O binding energy. Although reduction of both by the 4 kV Ar ion beam is evident, it is safe to assume that the evaporated film is nearly stoichiometric[28] and chemically almost identical to sapphire.

The microstructure and diffraction pattern of Ti50Al after annealing at 700°C for 100s are seen in Fig. 13b as is the presence of a new aluminide phase, identified as TiAl. Table 6 gives its d-spacings and shows that they closely match those of standard TiAl (JCPDS file 5-678). The TiAl forms under conditions that keep the Al_2O_3/TiAl

interface stable: both TEM and XPS (not shown) indicate that there is no interfacial reaction at 700°C. We are thus able to form a 400 to 500Å-thick aluminide, sandwiched between two Al_2O_3 films or between Al_2O_3 and sapphire.

The diffraction patterns of Ti30Al and Ti70Al after the 700°C anneal are also listed in Table 6. The Ti-rich Ti30Al appears to consist of Ti_3Al (JCPDS fill #9-98) and some retained Ti. Many lines almost overlap in these two phases, and since the observed intensities differ greatly from those of Ti_3Al, and XPS indicates the presence of metallic Ti, we conclude that some Ti remains unreacted.

The Al-rich Ti70Al d-spacings appear to match well the recently calculated values for TiAl2[29]. In addition, in Ti70Al the d=1.99Å and 1.40Å sharp thin rings indicate the presence of extremely fine grained crystalline (c)-Al_2O_3. The crystallization of the a-Al_2O_3 film becomes evident in all specimens at 800°C. The a-Al_2O_3 to c-Al_2O_3 transformation occurs faster in the presence of Al-rich aluminides, which may provide excess Al to the Al_2O_3.

The diffraction pattern d-spacings of the three specimens after 100s at 800°C are listed in Table 7. Small changes in Ti30Al include the appearance of two c-Al_2O_3 lines.

The Ti50Al pattern, Fig. 13c, although basically similar to that at 700°C, shows additional lines. Two of these, at d=1.99 and 1.40Å belong to c-Al_2O_3. Others, at d=5.03, 2.52, 2.22 and 1.23Å, fit Ti_3Al (9-98) quite well, which would indicate a limited TiAl→Ti_3Al transformation and Al loss from the aluminide. However, the XPS profile (not shown) indicates that the Ti/Al ratio has not increased significantly, so the reaction at this temperature is quite limited.

The Ti70Al pattern remains unchanged from 700°C to 800°C, except that the c-Al_2O_3 lines are stronger at 800°C. **In summary, at 800°C all three aluminides seem to be stable.**

The d-spacings of polycrystalline phases in the three films after annealings at 900°C for 100s are given in Table 8, and are shown together with low magnification microstructures in Fig. 15 (Ti50Al is also shown in Fig. 13d). Changes from 800°C are seen in all three. In Ti30Al, the additional lines at d=2.57, 2.41, 2.27, 1.76, 1.48 and

1.37Å match Ti_2O (file #11-218) perfectly, and Ti_2O is a major phase in this specimen. Ti30Al also contains a few micron-size single crystals that appear to be either Ti_4O_7 or TiO_2 and that occupy 10-20% of the film area. These crystals sit in regions denuded of the former aluminide and probably represent the final product of the reaction.

The changes in the Ti50Al and Ti70Al patterns are interesting and difficult to explain at present. All lines in Ti50Al (except the Al_2O_3 reflections) fit the Ti_3Al pattern within ~1%. This would seem to continue the trend of a TiAl→Ti_3Al transformation, visible already at 800°C. Ti oxide single crystals appear only rarely in Ti50Al. The Ti-enrichment of the aluminide is confirmed in the XPS profile, Fig. 16a. The profile indicates an outdiffusion of Al from the aluminide and an indiffusion of O from the Al_2O_3 layer. More puzzling, the aluminide/Al_2O_3 interface, although wider than before, is still quite distinct, meaning that the "interfacial reaction" consists almost entirely of internal changes in the aluminide layer. A similar, and even more pronounced loss of Al and increase in O in the aluminide is evident in Ti50Al, Fig. 16b. Note that here the Al/O ratio in both Al_2O_3 film and sapphire is practically identical to that in the unannealed specimen, Fig 14a. Since 4kV Ar ion sputtering is certain to induce stoichiometry changes it is impossible to tell from the XPS profile how much if any of the Al leaving the aluminide stays in the oxide.

In Ti70Al, many lines match TiAl (5-678) very well and the pattern is very similar to that of Ti50Al at 800°C, except for the "thin lines" with d=2.29, 1.20 and 1.15Å which remain unassigned. If confirmed, the apparent $TiAl_2$→TiAl transformation in this sample implies, as in Ti50Al, the breakup of the aluminide and loss of Al. Ti oxide single-crystals were not detected in Ti70Al.

D. The TiAl/TiB_2 and TiAl/TiC Systems

The experimental procedure here followed exactly that in TiAl/Al_2O_3 films, except that no saphhire substrates were used. Details are given in ref. 11. All the as-deposited films show SAD patterns consisting of only Ti and Al lines. All four reinforcements are amorphous as- deposited. Table 9 lists the d-spacings after a low-temperature reaction (660°C, 5 min.) to form the aluminide: a complete AlTi (JCPDS file 5-678) pattern is seen in the TiAl/Al_2O_3 couple which was used for comparison. In addition, two strong lines with d=1.98Å and 1.40Å show the presence of crystalline

gamma-Al_2O_3. The TiAl/TiB_2 (b) and TiAl/TiC (c) patterns are composed mainly of TiB_2 and TiC lines, respectively, with only the strongest AlTi line at d=2.31Å visible. It is clear that all three amorphous reinforcements start to crystallize below 660°C when in contact with TiAl. There is no evidence for any reaction occurring between TiAl and Al_2O_3 under these conditions. However, in view of the much weaker AlTi patterns in the two other couples, it appears that they have undergone a reaction.

Table 10 lists the d-spacings of films annealed at 800°C for 5 minutes. Annealings at 900°C for 100s lead to the same results. The TiAl phase disappears in each case: in TiAl/Al_2O_3 couples, the reaction products are Ti_3Al (file 9-98) and gamma-Al_2O_3. After internal calibration using the gamma-Al_2O_3 line, the Ti_3Al spacings are within less than 1% of the file data. Reaction at 1000°C (unpublished) induces the formation of a small amount of Ti_2O (file 11-218).

In TiAl/TiB_2, the products appear to be a mixture of borides, possibly TiB + TiB_2. In TiAl/TiC, the main lines are those of TiC, with two very weak lines at d = 2.64 and 2.29Å indicating a minor Ti_2AlC (file 29-95) phase. There are no lines that can be attributed to TiAl in any of the films. **We thus see that on a nanometer scale TiAl is chemically incompatible with all three reinforcements at 1000°C, or even at a lower temperature if the times are long enough.**

IV. SUMMARY AND CONCLUSIONS

A. NiAl/MgO

We have found that NiAl will react with MgO at predicted operation temperatures. Even taking into consideration the possible differences between thin polycrystalline film and bulk reactivities, it is still likely that a limited interfacial reaction will occur in bulk composites, following roughly the same steps, and leading to the formation of a spinel and Ni_3Al. A limited nanoscale interfacial reaction, as pointed out, is not necessarily detrimental, as it may lead to strong bonding and therefore good mechanical strength. On a RELATIVE basis, when compared with other systems such as NiAl/ZrO_2, NiAl/Y_2O_3, NiAl/SiC, TiAl/Al_2O_3 and TiAl/MgO, investigated by the same method [8,15], **the MgO/NiAl reaction at 800°C is more limited, indicating that it is indeed one of the more stable aluminide-based IMC's.**

B. NiAl/Al_2O_3 and NiAl/ZrO_2

The changes observed in NiAl/ZrO_2 films cannot be solely attributed to NiAl oxidation by external oxygen, and therefore indicate a NiAl-ZrO_2 interfacial reaction, while those seen in NiAl/Al_2O_3 films are fully consistent with "external" oxidation. As reinforcements in NiAl-based IMC's, Al_2O_3 would rank as most stable, followed by MgO. ZrO_2 rates as less stable than both. Although bulk results with ZrO_2 are few and ambiguous[18],they also seem to indicate that it is a less stable reinforcement than Al_2O_3. The agreement in the stability rankings between thin-film and bulk couples is therefore quite good.

C. TiAl/Al_2O_3

The XPS comparison of the e-beam-evaporated a-Al_2O_3 film and sapphire before and after annealing, as well as other studies [28], indicate that the two are similar enough to consider a-Al_2O_3/intermetallic reactions as substantially equivalent to bulk c-Al_2O_3/intermetallic reactions. Moreover, layered Ti/Al films "sandwiched" between a-Al_2O_3 films form a Ti aluminide at 700°C, where the reaction with the

alumina film is negligible. The Ti/Al film reaction is probably similar to the exothermic reaction between Ti and Al powders at between 640 and 700°C reported recently[30]. Also, the formation of aluminides from thin Ti and Al films in the temperature range 350-700°C is well documented[31]. Thus we submit that the observations reported here can be considered as quite relevant to nanoscale interfacial reactions in real IMC's.

Regarding the nanoscale reactivity of Ti aluminides containing 30 to 70% (at.) Al we find that regardless of stoichiometry, all aluminides react with Al_2O_3. As expected, the reaction is faster (starts at lower temperature) for Ti-rich aluminides, in which it forms Ti oxides. At all compositions, it involves the indiffusion of O into the aluminide and its breakup, and the outdiffusion of Al. If the amount of material is finite (as in our films), one gets formation of more Ti-rich aluminides (i.e. $TiAl_2 \rightarrow TiAl$ and $TiAl \rightarrow Ti_3Al$ transformations), which, in the presence of increased O levels eventually decompose to form Ti oxides and partially oxidized Al. In our films, the Al that leaves the aluminide may diffuse through the oxide and reach the surface where it can be carried away by the Ar stream, a phenomenon observed also in bulk couples[7]. We emphasize that the interfacial reaction described here may be quite limited spatially. Nevertheless, in the context of its possible influence on the IMC properties it could be important.

While keeping in mind the difference between thin, finite reaction couples and infinite bulk couples, we find that for contents of less than the gamma (50%) composition, our results are in agreement with some bulk results[7] but contradict others[21,22]. Specifically, Misra [7] demonstrates that bulk Ti-54%Al/Al_2O_3 couples do not react even at 1300°C after 66 hours. Decock et al.[21] find similar stability of gamma-$TiAl_2O_3$ couples at 1100°C after 192 hours. For Al-rich aluminides our results basically disagree with all published experimental data [e.g 7,22,32] as well as with predictions of recent Ti-Al-O phase diagrams[21,33]. **We conclude that on a nanometer scale, Ti aluminides and Al_2O_3 are not chemically compatible, and that aluminides with 30-70% Al lose their Al and transform first into more Ti-rich aluminides and eventually into Ti oxides.**

D. TiAl/TiB_2 and TiAl/TiC

Our study is showing extensive nanoscale reactivity in these couples. To understand these results, one has to look at the possible reactions as well as the mechanisms by which such reactions may occur. Regarding the predicted unstable TiAl/TiC system, the following reaction

$$TiAl + TiC \rightarrow Ti_2AlC \quad (3)$$

is favored thermodynamically[34,35]. The very weak Ti_2AlC reflections indicate that it does indeed occur. The strong TiC lines at 900°C are due to excess TiC. The relative amount of TiAl and reinforcement "molecules" in each specimen can be calculated approximately using the film thicknesses, bulk density values and atomic or molecular weights. The molecular ratio is found from the formula:

Layer #1 thickness x density / molecular weight
Layer #2 thickness x density / molecular weight

Assume that volume changes during formation of TiAl from Ti and Al are accommodated fully by changing only the thickness; therefore, 252Å Al + 265Å Ti will form a 480Å TiAl layer. By using bulk densities (in g/cm^3) and molecular weights of 3.9 and 74.88 for TiAl, 3.9 and 101.96 for Al_2O_3, 4.5 and 69.54 for TiB_2, and 4.9 and 59.91 for TiC, respectively, we find the following molecular ratios: a) $TiAl/Al_2O_3$ = 25/23; b) $TiAl/TiB_2$ = 25/39; and c) TiAl/TiC = 25/32; thus it is clear that excess TiC will exist after the entire TiAl layer is consumed in reaction 1. Regarding the other two systems, possible reactions are:

$$9TiAl + Al_2O_3 \rightarrow Ti_3Al + 10Al + 3Ti_2O \quad (4)$$

$$TiAl + TiB_2 \rightarrow 2TiB + Al \quad (5)$$

The lack of thermodynamic data on Ti_2O precludes a definitive check on the validity of reaction (4). In accordance with the molecular ratios calculated above, excess Al_2O_3 as well as excess Al should be seen in the $TiAl/Al_2O_3$ couple. The strong gamma-Al_2O_3 lines provide evidence of Al_2O_3 existence, but Al lines are never seen. However, we mentioned above that X-ray photoelectron spectroscopy (XPS) profiles of $TiAl/Al_2O_3$ couples show that Al from the aluminide layer diffuses out, crosses the thin Al_2O_3 layer and evaporates, being swept from the specimen surface by the flowing

argon[7], thus explaining the missing pattern. As an interesting aside, the observed reactivity of TiAl with Al_2O_3 may explain its oxidation behavior. When a lamellar TiAl/Ti_3Al structure is oxidized[36], Al_2O_3 "paths" initiate from the TiAl area, suggesting that aluminum to form Al_2O_3 is mainly supplied to the lamellar boundaries from the Al-rich TiAl phase. Such outdiffusion of Al from TiAl matches our observations exactly[8].

Regarding reaction (5), calculated phase equilibria for the system Ti-Al-B at 1100°C[21] indicate that it should be favored thermodynamically: a tie line exists between gamma-TiAl and TiB but not between gamma-TiAl and TiB_2. The molecular ratios clearly show that excess TiB_2 should be present after total consumption of the TiAl layer. Missing Al lines may again be attributed to its outdiffusion.

In summary, this study strongly suggests that the likelihood of nanoscale interfacial reactions in "stable" systems is greater than anticipated. This finding appears to contradict existing evidence of BULK non-reactivity in most of these systems (except TiAl/TiC). There may be a number of reasons for this apparent contradiction between bulk and thin-film results. For example, the resolution of the techniques used in bulk studies may be too poor to detect nanometer-scale reaction products; the reactions may be self limiting, with the product phase becoming an efficient diffusion barrier preventing further layer growth. Thin-films may differ chemically from bulk, affecting the reactivity, although comparisons of TiAl (film) reactions with thin Al_2O_3 films and with sapphire show that if anything, the sapphire is more reactive [8]. We suggest however that the existence of nanoscale reactions at supposedly "stable" interfaces should be considered the norm, rather than the exception, particularly at the high temperatures of IMC preparation or use.

V. REFERENCES

1. "Composite Materials", vol. 1, A.G.Metcalfe, ed., Academic Press, 1974.
2. A.G. Metcalfe, ibid, p.1.
3. A.G. Metcalfe, ibid, p.65.
4. R.E.Tressler, ibid, p.286.
5. W. Bonfield, ibid, p.364.
6. A.K.Misra, NASA Contractor Report 4171, 1988.
7. A.K. Misra, Metall. Trans. A, 22A (1991) 715.
8. M. Nathan, C.R.Anderson and J.S.Ahearn, Mater. Sci. Eng. A162 (1993) 107.
9. M. Nathan and J.S.Ahearn, J. Mater. Sci. Lett. accepted for publication.
10. M. Nathan, C.R.Anderson and J.S.Ahearn, J. Mater. Sci., accepted for publication.
11. M. Nathan and J.S. Ahearn, J. Mater. Sci. Lett. 12 (1993) 1622
12. M. Nathan and J.S.Ahearn, J. Appl. Phys. 70 (1991) 811.
13. Joint Committee on Powder Diffraction Standards, "Powder Diffraction File" International Center for Diffraction Data, Swarthmore, PA, 1985.
14. J. Doychak, J.L.Smialek and T.E.Mitchell, Met. Trans. 20A (1989) 499 and references thereof.
15. M. Nathan, unpublished.
16. M. Bobeth, W.Pompe, E.Schumann and M.Ruhle, Acta. Metall. Mater. 40 (1992) 2669.
17. J.Doychak, J.A.Nesbitt, R.D.Noebe and R.R.Bowman, Oxid. Met. 38 (1992) 45.
18. J.D.Rigney and J.J. Lewandowski, J. Mater. Sci. 28 (1993) 3911.
19. C.A.Anderson, J.Greggi,Jr.,and T.K.Gupta,in "Advances in Ceramics", vol.12, edited by N. Claussen, M. Ruhle and A.H. Heuer (The American Ceramic Society, Columbus, OH, 1984), p. 78.
20. E.C.Subbarao in "Advances in Ceramics", vol. 3, edited by A.H. Heuer and L.W.Hobbs (The American Ceramic Society, Columbus, OH, 1981), p. 1.
21. J.A. Decock, Y.A. Chang, M.-X. Zhang, and O.Y. Chen, MRS Symp. Proc. 170 (1990) 173.
22. D.S. Shih and R.A. Amato, Scripta Metall. et Mater., 24 (1990) 2053.
23. J.H. Selverian, F.S. Ouchi, M. Bortz, and M.R. Nottis, J. Mater. Sci., 26 (1991) 6300.
24. R.E. Tressler, T.L. Moore, and R.L. Crane, J. Mater. Sci., 8 (1973) 151.
25. X.-A. Zhao, E. Kolawa and M.-A. Nicolet, J. Vac. Sci. Technol., A4 (1986) 3139.
26. A. Rahmel and P.J. Spencer, Oxidation of Metals, 35 (1991) 53.
27. H. Lefakis, M. Liehr, G.W. Rubloff, and P.S. Ho, MRS. Symp. Proc., 54 (1986) 134.
28. A.K. Dua, V.C. George, and B.P. Agarwala, Thin Solid Films, 165 (1988) 163.
29. H. Mabuchi, T. Asai and Y. Nakayama, Scripta Metall . 23 (1989) 685.
30. W.R. Wrzesniski and J.C. Rawers, J. Mater.. Sci. Lett., 9 (1990) 432.
31. L.R. Parks, D.A. Lilienfeld, P. Borgesen and R. Raj, MRS Symp. Proc. 213 (1991) 925 and references thereof.
32. S. Krishnamurty in "Interfaces in Metal-Ceramic Composites," R.Y. Lin, R.J. Arsenault, G.P. Martins and S.G. Fishman, eds., TMS 1989, p. 75.

33. S.K. Choi, F.J.J. Van Loo and R. Metselaar, British Ceram. Proc. 48 (1991) 123.
34. J.H.Norman, G.H. Reynolds and L. Brewer, MRS Symp. Proc. 194 (1990) 369.
35. J.C. Schuster, H. Novotny and S.C. Vaccaro, J. Solid State Chem. 32 (1980) 213.
36. A. Takasaki, K. Ojima, Y. Taneda, T. Hoshiya and A. Mitsuhashi, Scripta Metall. et Mater. 27, 401 (1992).

INVESTIGATION OF BULK INTERFACIAL REACTIONS WITH THIN-FILM MODELS

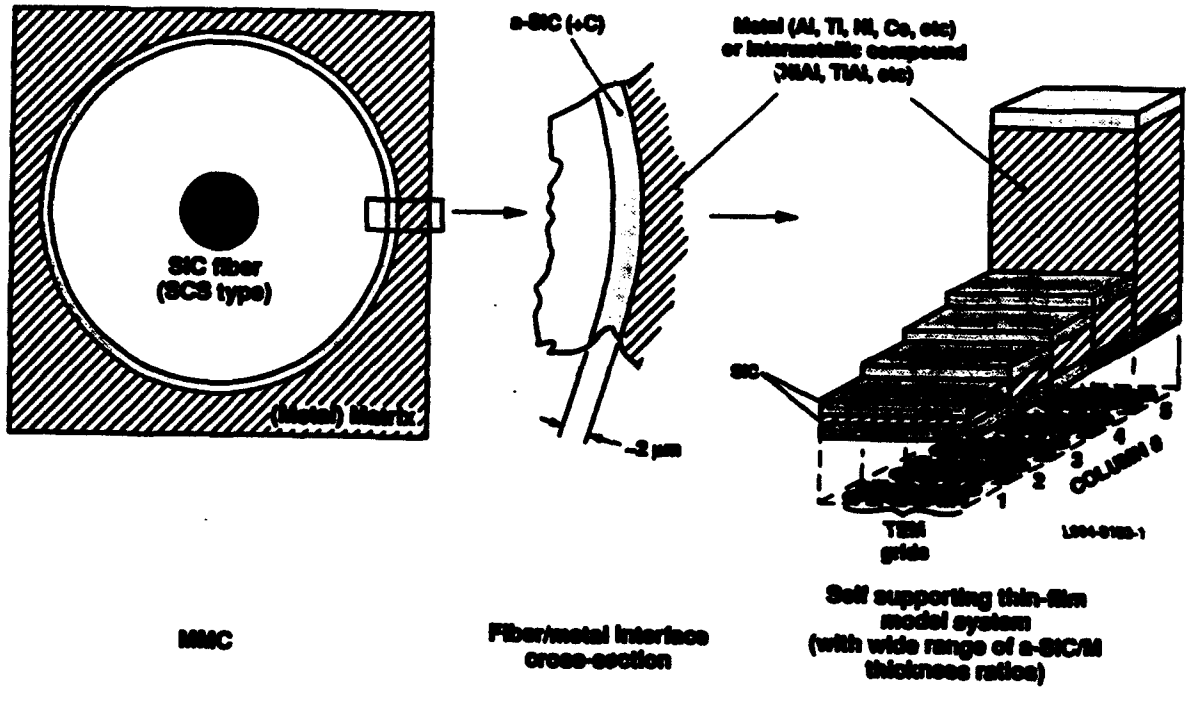

Figure 1. Investigation of bulk interfacial reactions with thin-film models. Although the specific drawing describes a SiC fiber/matrix system, it can of course be considered general.

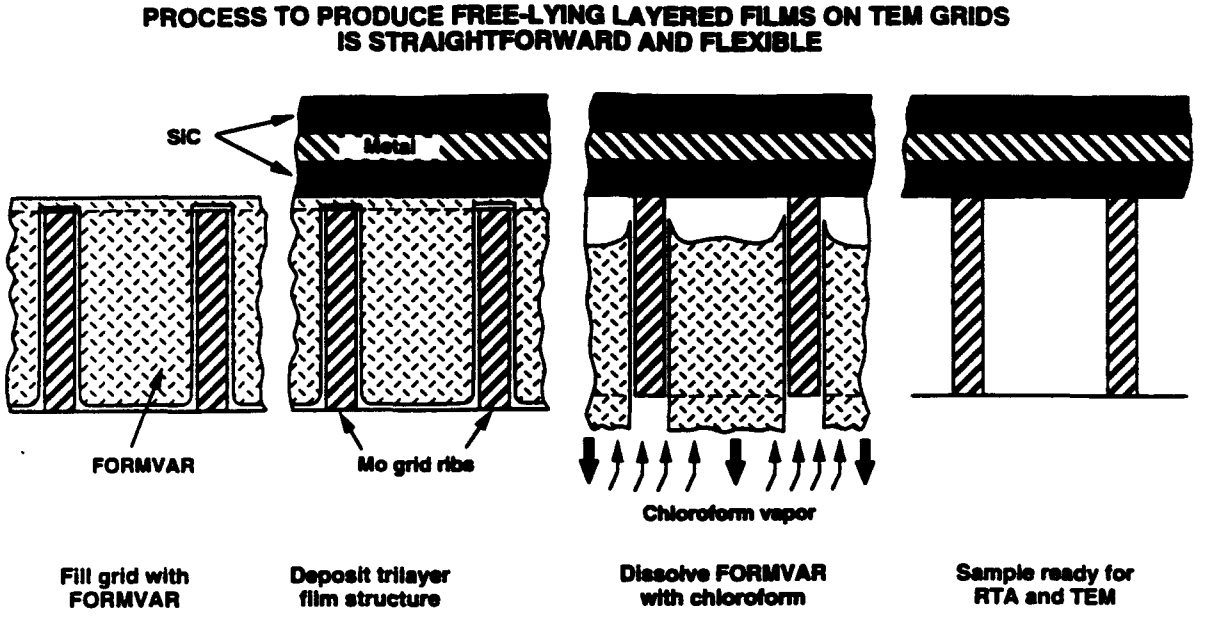

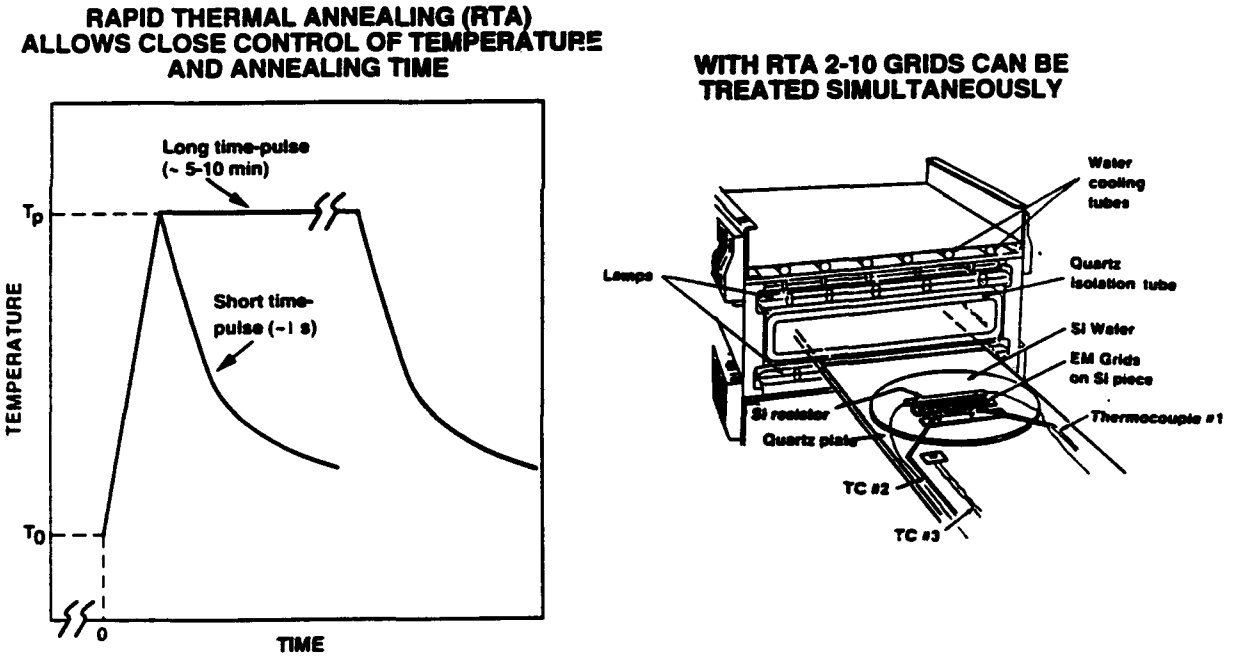

Figure 2. Schematic description of the steps in the preparation of layered films-on-grid, typical rapid thermal annealing T-t curves, and the annealing procedure.

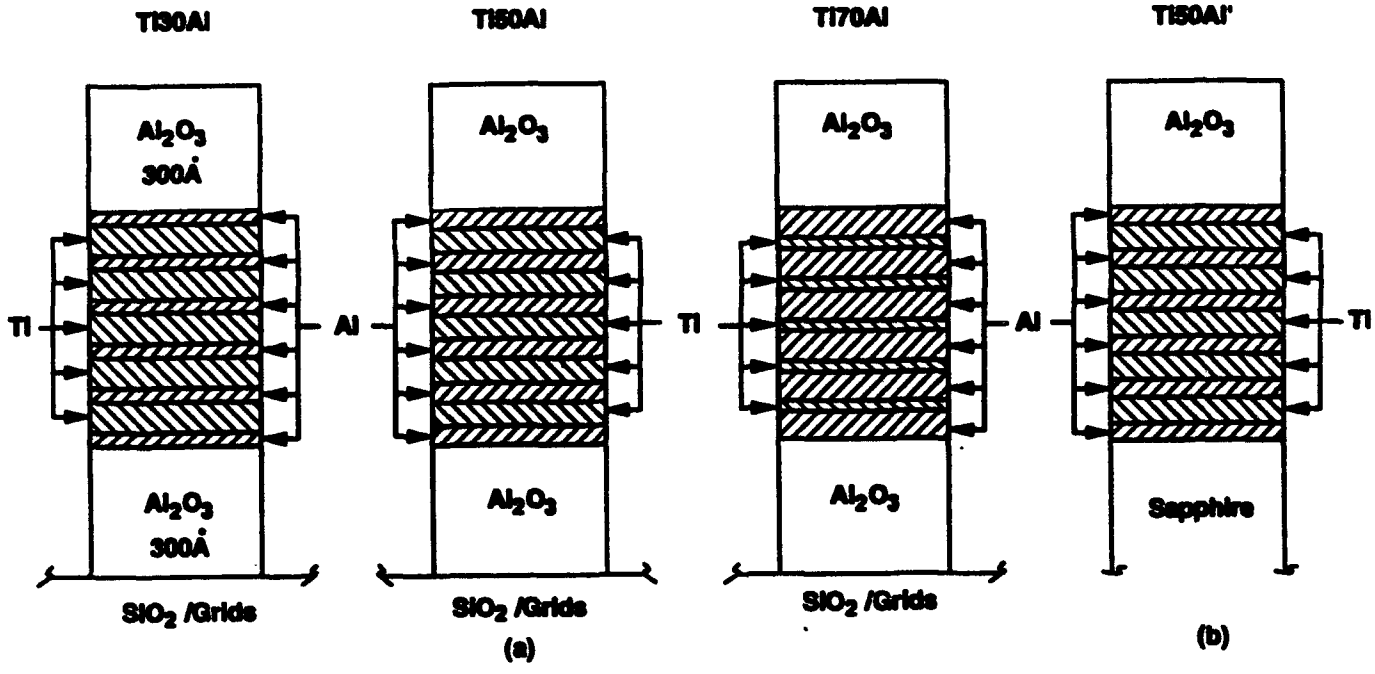

Figure 3. Schematic description of the layered films used in this study: (a) Al_2O_3/Ti aluminide/Al_2O_3 structures with three different Ti/Al ratios in the aluminide; (b) Al_2O_3/Ti50Al/sapphire structure. Al/Ti/Al. layer thicknesses:

Ti30Al - 30/74/23/74/23/74/23/74/23/74/30Å;
Ti50Al and Ti50Al' - 42/53/42/53/42/53/42/53/42/53/42Å;
Ti70Al - 58/32/58/32/58/32/58/32/58/32/58Å.

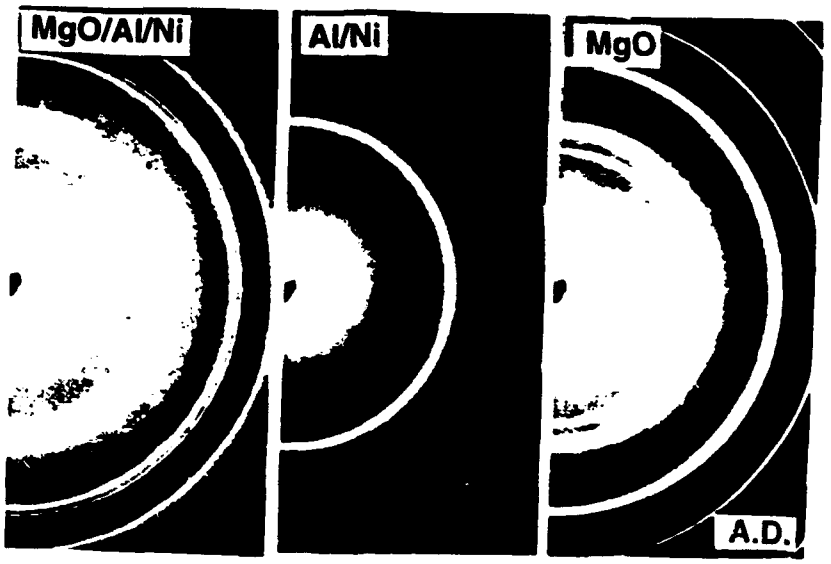

Figure 4. SAD patterns of as-deposited films.

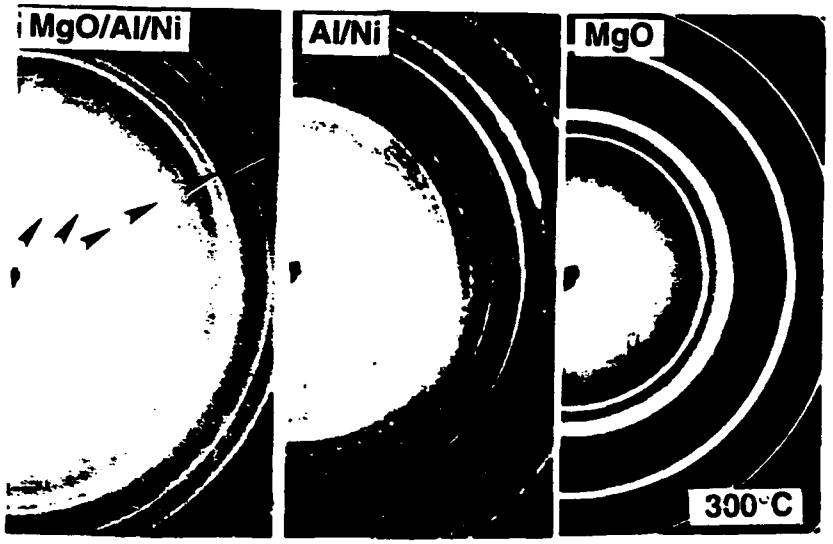

Figure 5. SAD patterns of films after annealing at 300°C for 100s.

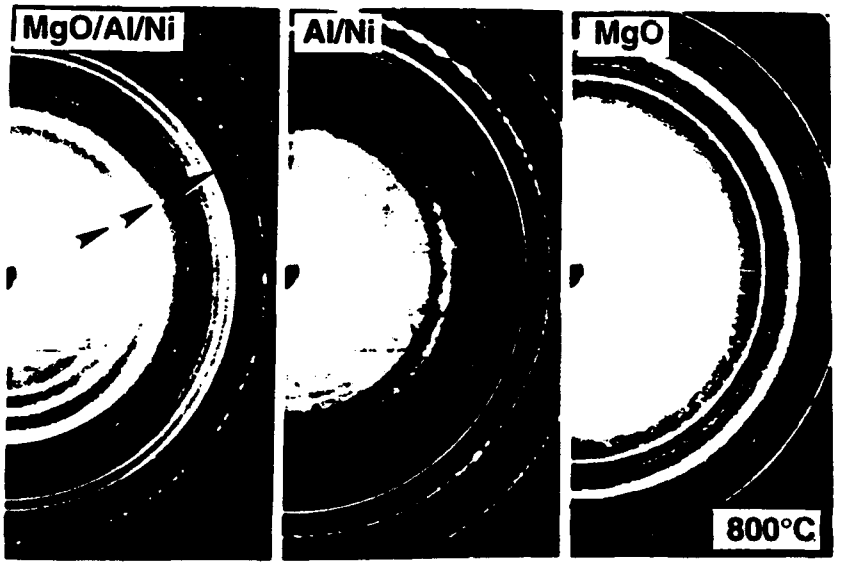

Figure 6. SAD patterns of films after additional annealing at 800°C for 5 minutes.

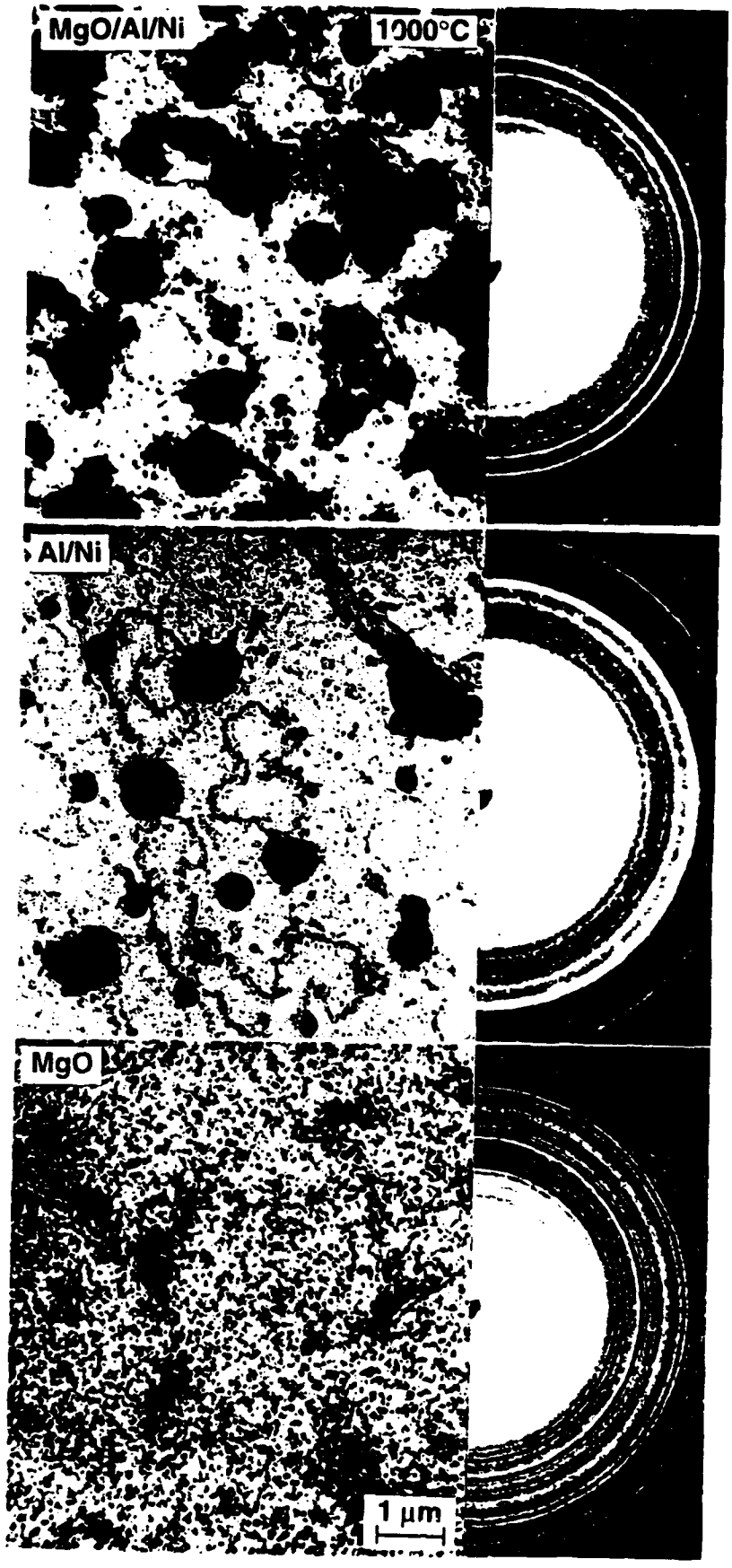

Figure 7. SAD patterns of films after additional annealing at 1000°C for 100s.

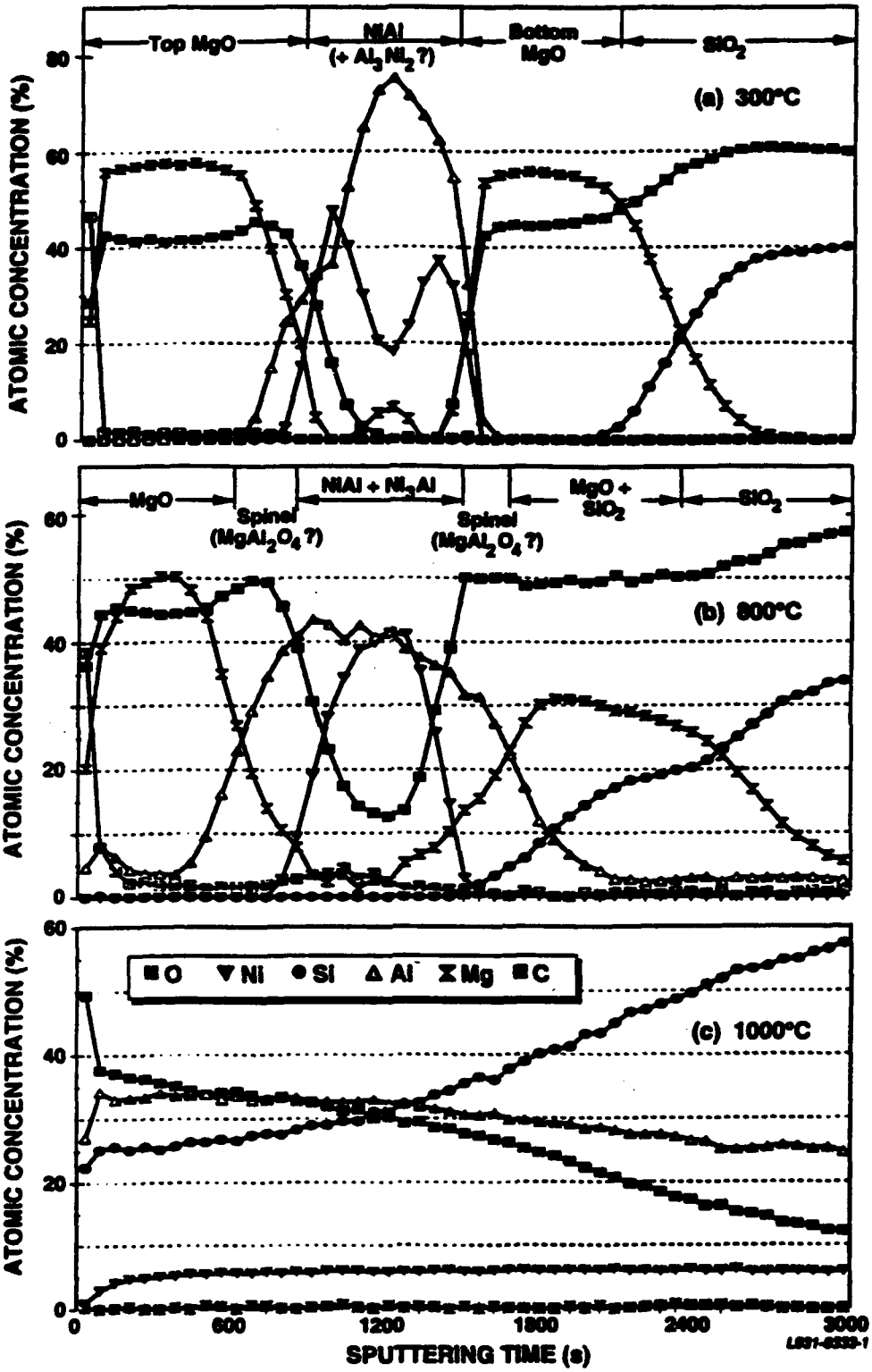

Figure 8. XPS depth profiles of films on oxidised Si substrates: a) after 300°C annealing; b) after additional 800°C annealing; c) after additional 1000°C annealing. The atom percentages have errors on the order of 5-10% due to uncertain sensitivity factors and overlapping peaks. "Negative" going signals caused by the signal procesing method (and obviously artifacts) have also been eliminated.

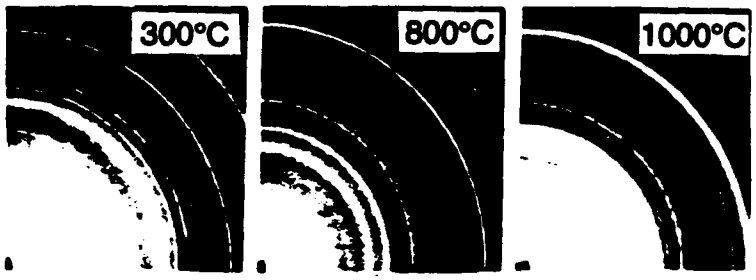

Figure 9. Electron diffraction patterns of $NiAl/Al_2O_3$ films annealed at 300°C for 5 minutes, then reannealed at 800°C for 5 minutes and 1000°C for 100s.

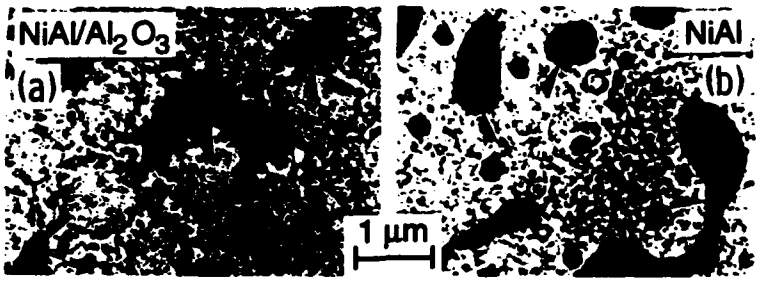

Figure 10. Microstructures after annealing at 1000°C: a) $NiAl/Al_2O_3$; b) NiAl film. Arrows in both point to Ni globules. The background is Al_2O_3.

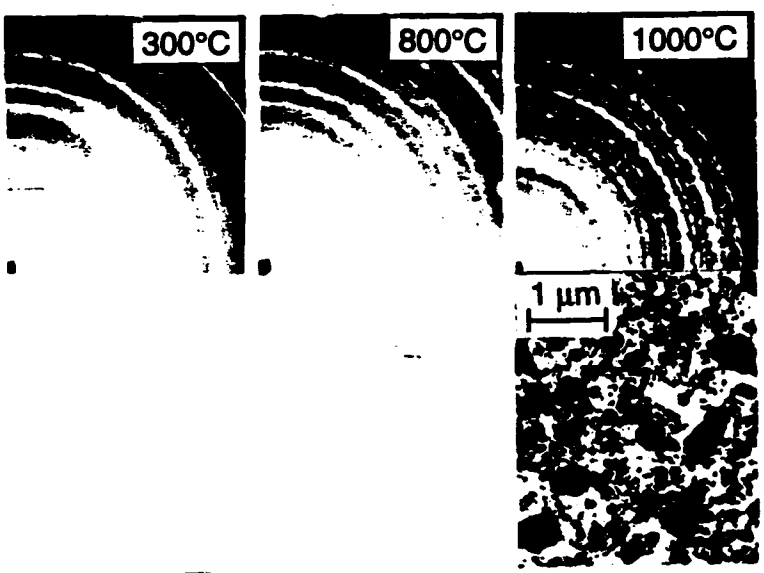

Figure 11. Electron diffraction patterns of $NiAl/ZrO_2$ films annealed at 300°C for 5 minutes, then reannealed at 800°C for 5 minutes and 1000°C for 100s. The microstructure at 1000°C exhibits voids (white areas) as well as Ni globules.

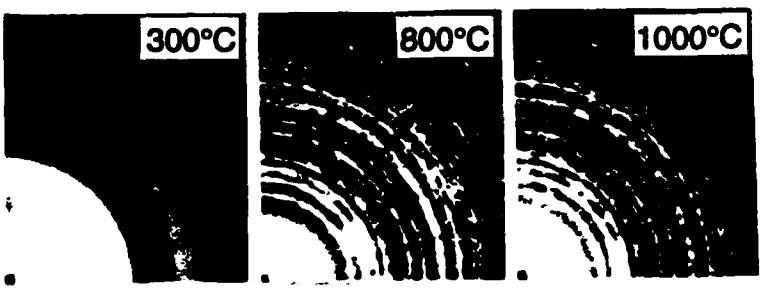

Figure 12. Electron diffraction patterns of a baseline 500A-thick ZrO_2 film, annealed simultaneously with the $NiAl/ZrO_2$ film. The structure is monoclinic at both 800 and 1000°C.

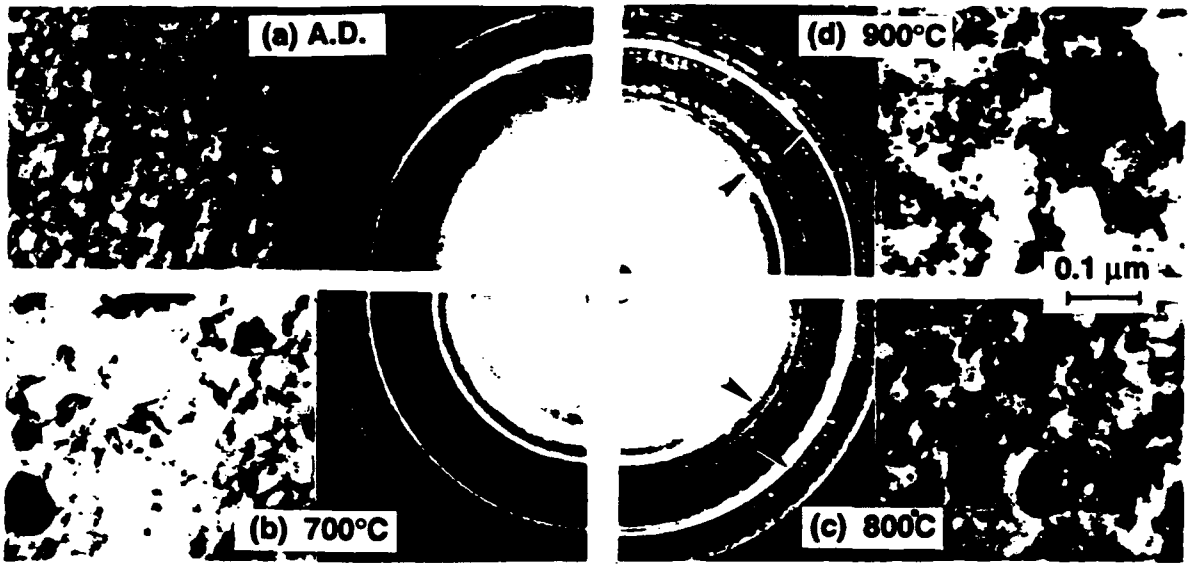

Figure 13. High magnification microstructures and diffraction patterns of Ti50Al: (a) as-deposited; and (b),(c),(d) - after 100s anneals at 700, 800 and 900°C respectively. Arrows in the diffraction patterns indicate c-Al_2O_3 reflections.

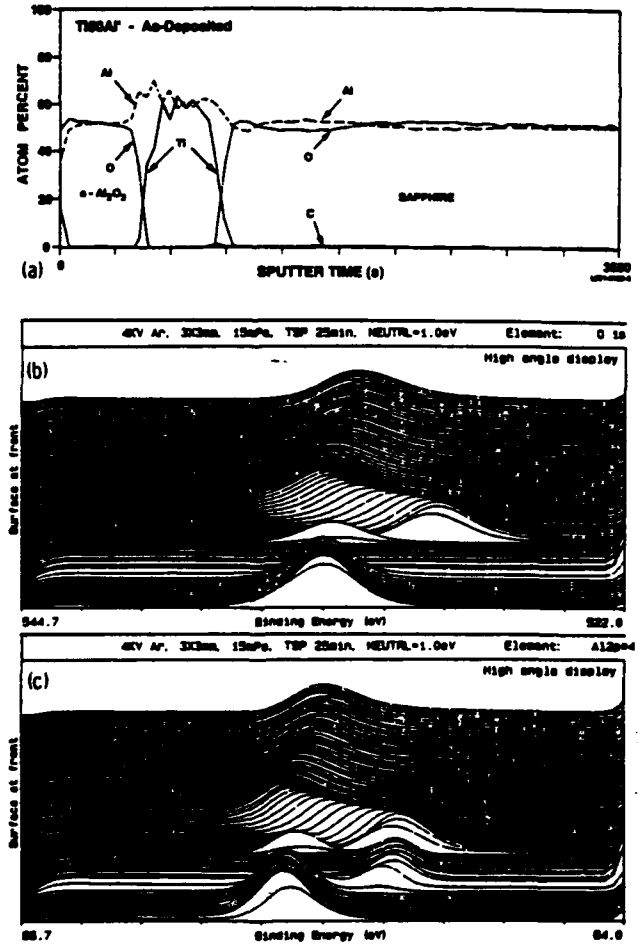

Figure 14. (a) XPS profile, (b) O1s scans and (c) Al2p scans of the as deposited a-Al_2O_3/Ti50Al/sapphire structure. Note the almost identical O/Al ratio in the a-Al_2O_3 film and the sapphire substrate. The energy shifts in the sapphire are artifacts due to the sputtering process, as is the apparent oxide substoichiometry.

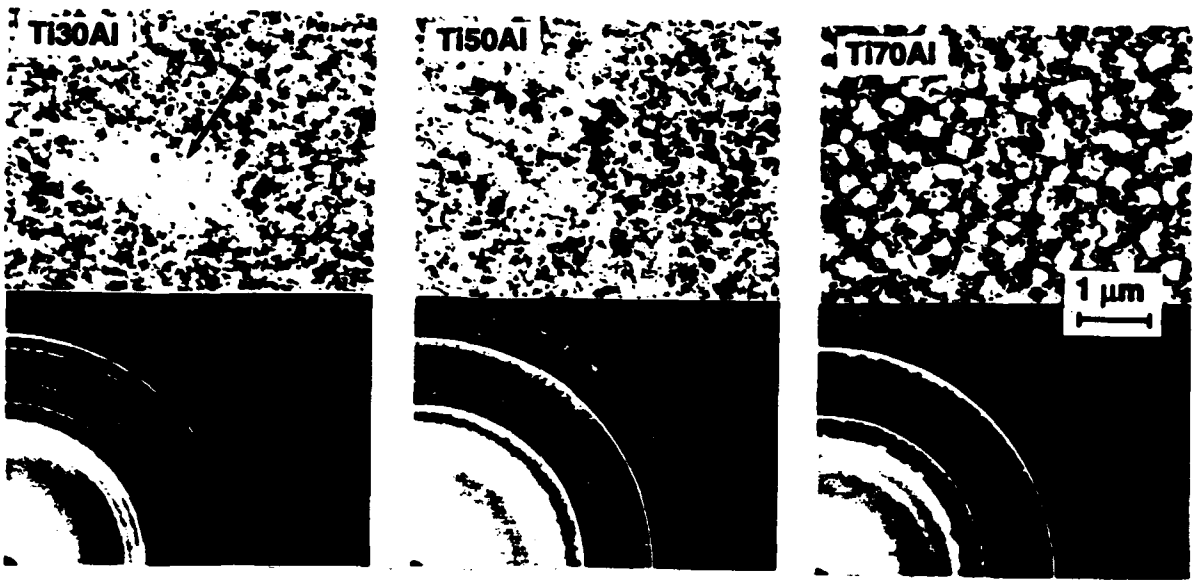

Figure 15. Low magnification microstructures a nd diffraction patterns of the three specimens after 100s anneals at 900°C. A single crystal Ti oxide region in Ti30Al is indicated by an arrow.

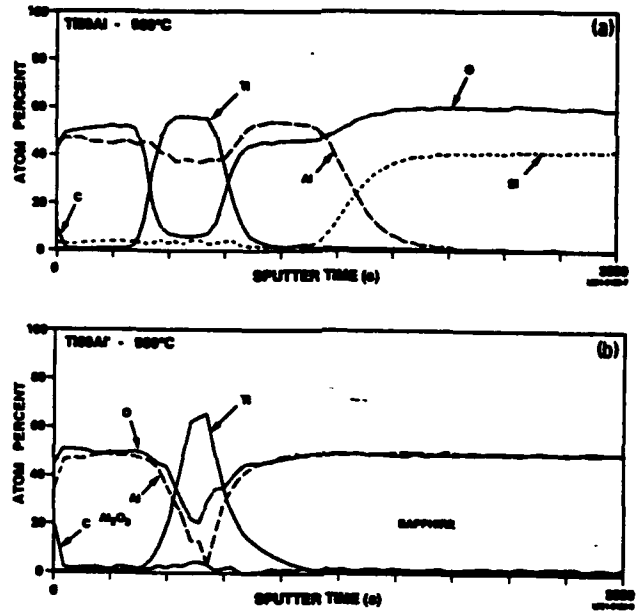

Figure 16. XPS profiles of 900°C annealed films: (a) Ti50Al; (b) Ti50Al'. The loss of Al from the aluminide layer is clear, particularly in Ti50Al'. Also evident is the diffusion of O into the aluminide. Due to sputtering effects and background correction uncertainties the exact stoichiometry in each layer is unknown. However, the error in the aluminide is not likely to be greater than a few percent.

TABLE 1. Al/Ni layer thicknesses (in Angstroms) for the NiAl/MgO study. Top and bottom layers are 300A-thick MgO. The thicknesses yield an equiatomic NiAl compound.

MgO	Al	Ni	Al	Ni	Al	Ni	Al	Ni	Al	Ni	Al	MgO
300	50	40	50	40	50	40	50	40	50	40	50	300

TABLE 2. Interplanar spacings of films annealed at 300°C for 100s + 800°C for 300s. Intensity notations: s- strong, m - medium, w - weak, v - very. * - possible NiO reflections.

Al/Ni	MgO	MgO/Al/Ni	Comments
dotted rings	solid rings	solid rings	
2.54ms	5.12vw	4.68vvw	spinel?
2.07vs	3.92m	3.94vvw	MgO
1.78vvw	3.75vw	2.84w	Al Ni or NiAl
1.60mw	3.49w	2.44s	MgO
1.47mw*	3.01m	2.11s	MgO
1.27vs	2.52m	2.01s	Al Ni or NiAl
1.20w*	2.45s		
1.08vs	2.27w	1.49s	MgO
	2.11vs	1.42s	Al Ni or NiAl
	1.75m	1.23w	MgO
	1.68vvw		
solid rings	1.64vw	dotted rings (trace)	
	1.49vs		
2.76vw	1.40vw	2.05vvw	Ni Al
2.41vw	1.35w	1.78vw	*
1.98vw	1.32vvw	1.26s	*
1.40vs	1.22m	1.07m	*
	0.94s	0.81m	*

TABLE 3. Interplanar spacings of the films in Table 2, further annealed at 1000°C for 100s. Same notations as in Table 2.

Ni/Al*	MgO	MgO/Al/Ni
solid ring	dotted rings	semi-solid rings
1.40vs	5.11m	4.68w
	4.33vw	2.88m
	3.90s	2.44s
	3.73m	2.02s
	3.49s	1.66vw
		1.55m
	3.02m	1.43s
	2.79s	
	2.52s	dotted rings (trace)
	2.48m	
	2.27m	5.13w
	2.17s	3.92m
	2.03vw	3.49m
	1.95vw	2.78m
	1.89vw	2.52m
	1.75vs	2.32m
		2.18w
		1.75s

* Due to the fuzziness of the lines, accurate spacings are unavailable and the phases cannot be identified.

TABLE 4. Interplanar spacings of NiAl/Al_2O_3 films annealed at various temperatures. Same notations as in Table 2.

300°C, 5 min	Comments	+800°C, 5 min	Comments	+1000°C, 100s	Comments
dotted lines		dotted lines			
4.85s	Al_3Ni_2	2.88m	NiAl	6.56w	Lines identical to
3.48s	"	2.04s	"	4.50w	those is a 500Å
2.85s	"	1.66w	"	4.03w	Al_2O_3 film
2.44w		1.44m	"	3.28m	
2.00vs	"	1.29vw	"	3.02vw	
1.87s	"	1.18vs	"	2.78s	
1.74s				2.73s	
1.64w		solid lines		2.60m	
1.48w				2.45vs	
1.42s	"	4.50vvw	γ-Al_2O_3	2.28s	
1.33vw		2.40m	"	1.98s	
1.27vw		2.28m	"	1.97s	
1.16s	"	1.99m	"	1.62w	
1.15s	"	1.52vw	"	1.50w	
		1.39vs	"	1.41vvs	
		1.14m	"	1.40vvs	

TABLE 5. Interplanar spacings of NiAl/ZrO_2 films annealed at various temperatures. Same notations as in Table 2.

300°C, 5 min	Comments	+800°C, 5 min	Comments	+1000°C, 100s	Comments
solid (*) + doted lines		doted lines			
2.91s	t-ZrO_2	2.90s	t-ZrO_2	Combination of t and m-ZrO_2 lines,	
2.88w	NiAl	2.55m	"	with no evidence of either aluminides	
2.56mw	ZrO_2	2.50m	"	or Al_2O_3. Many lines overlap those	
2.53mw	"	2.06vw		of a 500Å ZrO_2 film.	
2.08vw	"	2.01vvw			
2.02s*	NiAl	1.17s	"		
1.80s	ZrO_2	1.53m	"		
1.65vvw	NiAl	1.51m	"		
1.55m	ZrO_2	1.45vvw	"		
1.52m	"				
1.17s*	"	solid lines			
		2.69vvw	ZrO		
		2.33vvw	"		
		1.66vvw	"		
		1.40vvw	"		
		dots			
		2.07	Ni_3Al		
		1.27	"		

TABLE 6. Experimental d-spacings of films-on-grid after 700°C, 100s RTA; standard patterns with the closest match are listed for comparison.

Ti30Al	$AlTi_3$ file 9-98	Comments	Ti50Al	AlTi file 5-678	Ti70Al	$TiAl_2$ (ref. 11)	Comments
5.05ms	5.010_{10}						
			4.06w	4.070_{20}	3.96w	$3.916_{7.4}$	
2.90vvw	2.880_5		2.84m	2.810_{20}	2.74vvw	$2.733_{2.9}$	
2.53vs	2.500_{50}	Ti?					
2.35w	2.320_{70}	Ti?	2.32vs	2.310_{100}	2.32vs	2.305_{100}	
2.23m	2.205_{100}	Ti?					
			2.01s	1.990_{60}	2.01m	$2.026_{14.1}$	
					1.99m,d	$1.984_{33.5}$	
					1.99m,c		Al_2O_3
1.91vw	1.886_5	?					
			1.81w	1.790_{10}	1.78w	$1.770_{1.1}$	
			1.66w	1.650_{10}			
1.46s	1.474_5	Ti?	1.43s	1.424_{60}	1.42s	$1.418_{16.0}$	
			1.41w	1.407_{20}	1.41s,c		Al_2O_3
1.26m	1.251_{10}	Ti?					
1.22m	1.227_{40}	Ti?	1.21w	1.203_{60}	1.22s	$1.217_{7.3}$	
			1.16m	1.159_{20}	1.21s	$1.200_{21.6}$	

Experimental intensity notations: s strong, m medium, w weak, v very, d dotted, c continuous.

TABLE 7. Experimental d-spacings of films-on-grid after 800°C, 100s RTA.

Ti30Al	Comments	Ti50Al	Comments	Ti70Al	Comments
5.05ms					
		5.03vvw			
		4.06w			
2.90vvw		2.84m		2.74vvw	
2.52vs		2.52vw			
		2.33vs		2.32vs	
2.22m		2.22mw			
		2.05m			
		1.99m		1.99m	
1.98m,c	Al_2O_3	1.98m,c	Al_2O_3	1.98s	Al_2O_3
1.91vw					
		1.81vvw		1.78w	
		1.67vvw			
1.46m		1.43m		1.43s	
				1.41s,d	
1.40s,c	Al_2O_3	1.40s,c	Al_2O_3	1.41s,c	Al_2O_3
1.26w					
1.24w		1.23m		1.22s	
1.22m		1.21m		1.21s	

TABLE 8. Experimental d-spacings of polycrystalline phases in films after 900°C, 100s RTA; single-crystal reflections in Ti30Al are not listed.

Ti30Al	Comments	Ti50Al	Comments	Ti70Al	Comments
5.05w		5.05vvw			
				4.09w	
		3.44m		3.44vvw	
				2.84m	
2.57s					
2.53s		2.52s			
2.41vw		2.40w,c	Al_2O_3	2.40m,c	Al_2O_3
2.38vw					
		2.33s		2.33s	
				2.29w,c	Very thin line
2.27s					
2.23m		2.23m		2.23m	
1.99c	Al_2O_3	1.98c	Al_2O_3	1.99c	Al_2O_3
		1.91vw			
		1.83vw		1.80vvw	
1.76m		1.76vvw			
		1.73m		1.72vvw	
				1.66vw	
1.48s		1.49vvw			
1.46m		1.46w		1.44m	
1.40c	Al_2O_3	1.40c	Al_2O_3	1.41c	Al_2O_3
1.37vw		1.34m		1.34w	
1.26w		1.26m			
1.24w		1.24m		1.23m	
1.22m		1.22m		1.22s	
				1.20w,c	Very thin line
				1.15m,c	Very thin line

TABLE 9. Interplanar spacings of films annealed at 660°C for 5 min.

TiAl/Al_2O_3 *d* (nm)	TiAl/TiB_2 *d* (nm)	TiAl/TiC *d* (nm)
0.409 m[a]	0.323[b] vvw	0.281 vvw
0.283 m	0.282 vw	0.259 vvw?
0.232 vs	0.249 vw	0.249[b] s,c
0.205 w	0.231 vs	0.231 s
0.201 w	0.215 vw?	0.227 w
0.198[b] m,c	0.198 m	0.215[b] s,c
0.179 w	0.168 vvw	0.200 vw
0.166 vw	0.150[b] w	0.153[b] s,c
0.143 s	0.141 m	0.143 w
0.139[b] s,c	0.138[b] vvw	0.139 w
0.134 vvw	0.120[b] w	
0.127 vvw		
0.122 m		
0.121 ms		
0.116 w		

[a]s, Strong; m, medium; w, weak; v, very; c, continuous; ?, unidentified. [b]Reinforcement reflection.

TABLE 10. Interplanar spacings of films annealed at 800°C for 5 min.

$TiAl/Al_2O_3$ d (nm)	$TiAl/TiB_2$ d (nm)	TiAl/TiC d (nm)
0.505 vw[a]	0.263 m	0.264 vvw
0.343 m	0.250 s	0.250 vs
0.290 vvw	0.216 s	0.229 vvw
0.274 w,c?	0.204 m,d	0.215 s
0.251 s	0.153 vs	0.153 vs
0.239[b] m,c	0.140 w	0.131 m
0.236 s	0.131 vw	0.125 mw
0.227 m,c?	0.125 vw	0.099 mw
0.222 s	0.122 vw,d	0.097 m
0.198[b] s,c	0.104 vw	
0.190 vvw	0.096 w	
0.182 vw		
0.175 vvw		
0.171 s		
0.148 w		
0.145 m		
0.140[b] vs,c		
0.136 vw		
0.132 s		
0.125 m		
0.123 m		

[a]Notation as in Table II except d, diffuse and [b]γ-Al_2O_3.